

“Sweet Chemistry”: a Green Way for Obtaining Selenium Nanoparticles Active against Cancer Cells

Adriana P. Vieira,^{*a} Erika M. Stein,^b Daniel X. Andreguetti,^c Gerardo Cebrián-Torrejón,^{a,c} Antonio Doménech-Carbó,^c Pio Colepicolo^d and Ana Maria D. C. Ferreira^a

^a*Departamento de Química Fundamental, Instituto de Química and*

^b*Departamento de Análises Clínicas e Toxicológicas, Faculdade de Ciências Farmacêuticas, Universidade de São Paulo, Av. Prof. Lineu Prestes, 03178-200 São Paulo-SP, Brazil*

^c*Department de Química Analítica, Facultat de Química, Universitat de València, Dr. Moliner 50, 46100 Burjassot, Valencia, Spain*

^d*Departamento de Bioquímica, Instituto de Química, Universidade de São Paulo, Av. Prof. Lineu Prestes, 748, 05508-000 São Paulo-SP, Brazil*

We present an environment friendly synthesis of selenium nanoparticles and the study of their cytotoxic activity against uterine sarcoma cancer and fibroblasts cells. Amorphous selenium (a-SeNPs) and trigonal selenium (t-SeNPs) were synthesized using *D*-fructose as the reducing agent and characterized by high-resolution transmission electron microscopy (HRTEM), energy-dispersive X-ray spectroscopy (EDX), powder X-ray diffraction analysis (XRD), inductively coupled plasma optical emission spectrometry (ICP OES), dynamic light scattering (DLS) to obtain zeta potential values and cyclic voltammetry (CV). Particularly, a-SeNPs presented high toxicity toward the resistant cancer cell line MES-SA/Dx5 and its parental MES-SA line. However, they are not toxic against P4 fibroblast cells in comparative studies.

Keywords: selenium nanoparticles, *D*-fructose, cancer cells, green chemistry, cytotoxicity

Introduction

Selenium is an essential element of significant importance not only for humans, but also for other forms of life.^{1,2} Inorganic seleno-compounds have strong antioxidant activity, as well as some pro-oxidant effects and, additionally, have great importance in nutrition and medicine.^{3,4} Epidemiological studies have already demonstrated the potential role of selenium in the prevention and treatment of cancer cells.⁵⁻⁷ For example, selenium supplementation showed effective reduction in the incidence of cancer in the cervix, lung and liver.⁸ However, the biological activity of elemental selenium stands opposite to the selenium salts, since selenite and selenate showed inadequate cytotoxicity to normal cells.⁹⁻¹¹ In this sense, nanoparticles of elemental selenium stand out as an alternative, due to its low toxicity and acceptable bioavailability.¹²⁻¹⁴

Nanoparticles have become increasingly prominent in the medical field in the last few decades, giving rise to a new area, nanomedicine. This new area is focused on developing nanomaterials with potential use in therapy and diagnosis of diseases,¹⁵⁻¹⁷ including selenium nanoparticles (SeNPs).¹⁸

Generally, the methods for obtaining SeNPs involve multiple steps, high temperatures and pressures; require expensive equipment and reagents, as well as being harmful to the environment.¹⁹⁻²⁷ In this sense, it is necessary to develop simple routes that focus on green chemistry and no harm to the environment. Research has demonstrated the use of microorganisms such as bacteria, to reduce selenite. This method is considered a clean synthesis, but the cost and time of preparation of microbiological cultures is a disadvantage.²⁸⁻³⁰

The use of plant extracts and biopolymers such as chitosan, konjac glucomannan, gum acacia, carboxymethyl cellulose, sodium alginate and glutathione, as reducing agents of selenite has also been an alternative, since they are highly biodegradable and non-toxic materials. However, in each of these works there are several processing steps

*e-mail: apiresvieira@gmail.com

Conflict of interest: the University of São Paulo has filed patent (BR102016012928-1) relating to selenium nanoparticles synthesis and applications under study in the A. M. D. C. F. and P. C. laboratories.

until the attainment of SeNPs.³¹⁻³³

In this paper, we propose a method of synthesis of SeNPs that meet the principles of green chemistry, through a synthesis that requires little reaction time, non-toxic solvents, mild temperatures and uses a reducing agent that is biodegradable, cheap and not harmful to the environment. The use of sugars as reducing agents to obtain such nanoparticles has been investigated.³⁴⁻³⁶ Glucose and fructose have aldehyde and hydroxyl groups at carbon 1, respectively, which make them effective reducing agents. Researchers used glucose as a reducing agent and stabilizer of SeNPs; however, in their synthesis they used high temperatures and toxic solvents.^{35,36}

Therefore, we chose *D*-fructose because it is a plentiful and cheap reducing sugar to act as a reducing agent for sodium selenite in clean and quick synthesis of SeNPs using water as solvent and at low temperature. The obtained nanoparticles were tested for cytotoxicity against normal cells (fibroblasts-P4) and uterine sarcomas cells (MES-SA and MES-SA/Dx5) in order to assess their potential use as an anticancer drug.

Experimental

Preparation and characterization of selenium nanoparticles (SeNPs)

The SeNPs were prepared by the following procedure: an aqueous solution (1.0 mmol L⁻¹, 5 mL) of sodium selenite (Merck, Darmstadt, Germany) was slowly dripped in 10.0 mL of 1.0 mmol L⁻¹ aqueous solution of *D*-fructose (Merck, Darmstadt, Germany). The reaction mixture was then stirred, under heat at 45 °C for 15 min, when red staining nanoparticles were obtained (amorphous selenium, a-SeNPs), turning black after 20 min (trigonal selenium, t-SeNPs). Each solution containing selenium nanoparticles (a-SeNPs and t-SeNPs) was centrifuged at 13,000 rpm for 10 minutes. The pellets obtained were then re-suspended in deionized water and centrifuged again under the same conditions. This process was repeated three times for the removal of organic impurities present in SeNPs.

The nanoparticles free of organic impurities were quantified regarding selenium using an optical emission spectrometer with inductively coupled plasma (ICP OES) of Spectro, model Arcos. The energy-dispersive X-ray spectroscopy (EDX) analyses were obtained on a Shimadzu, EDX-720 model. The corresponding powder X-ray diffraction analysis (XRD) pattern was collected using a diffractometer with Cu K α operating at 30 kV, 15 mA, 5° to 2 θ = 90°, Rigaku, Miniflex model. The morphology and particle size were analyzed using a high-resolution

transmission electron microscope (HRTEM) JEOL, JEM 2100 model. The preparation of the samples consisted in dispersing the nanoparticles in a coated copper grid with a thin film of carbon, after careful drying with a filter paper. The grid was observed by HRTEM, using an accelerating potential of 200 kV. Measurements of the zeta potential were carried out by dynamic light scattering (DLS) using a Malvern, Zetasizer Nano model. Electrochemical experiments were performed at 298 \pm 1 K using potentiostat CH instruments, CH 660I model. A graphite bar (1 mm diameter) was used as working electrode, a platinum wire as auxiliary electrode and an Ag/AgCl (3 mol L⁻¹ NaCl) reference electrode completing the three-electrode arrangement. Voltammetry of microparticles experiments were performed at microparticulate films of amorphous selenium (a-SeNPs) and trigonal selenium (t-SeNPs) prepared by abrasively transferring a few nanogram sample onto the surface of the graphite electrode. Aqueous 0.25 mol L⁻¹ HAc/NaAc buffer solution at pH 4.75 was used as the electrolyte.

Cytotoxicity assays

For the *in vitro* studies of the cytotoxicity, the following cells were used: human foreskin fibroblasts isolated from tissue (cell P4), drug-sensitive human sarcoma cell line MES-SA and its multidrug-resistant (MDR) counterpart MES-SA/Dx5, as a model system for modulators' anti-MDR potency evaluation. P4 cells were maintained on Dulbecco's modified eagle medium (DMEM) containing 10% fetal calf serum, amphotericin B (0.63 μ g mL⁻¹) and penicillin (100 IU mL⁻¹), streptomycin (100 μ g mL⁻¹), at 37 °C, in a humidity-controlled incubator at 90% relative humidity and 5% CO₂. MES-SA cells were maintained on McCoy's 5A culture medium supplemented as above, and the MDR cell line MES-SA/Dx5 was cultivated at the same medium with doxorubicin 0.5 μ M, at 37 °C, in a humidity-controlled incubator at 90% relative humidity and 5% CO₂. After a few passages, cells were incubated at a concentration of 10 \times 10³ cell *per* well for drug exposition of 24 h in 96-wall plates, with a final volume of 100 μ L. After a period of 24 or 48 h, the cells were treated with concentrations 10 to 140 μ M of the a-SeNPs. The mortality cell assay was performed in duplicate, 24 h after starting exposure to drugs. The tetrazolium reduction assay (MTT) was performed in triplicate, according to the literature method.³⁷ Briefly, the medium was removed from the plates, the attached cells were washed with phosphate buffer solution and 200 μ L of the MTT solution were added to replaced culture medium, at a concentration of 500 μ g mL⁻¹. After an incubation period of 4 h at 37 °C, the MTT solution

was removed, and the formazan crystals were solubilized in 100 μL of DMSO. Absorbance of this formazan solution was measured with a Tecan Infinite M200 microplate reader (Männendorf, Switzerland), at a wavelength of 570 nm. The cell viability rate was estimated from the number of intact cells relative to the total number of cells in the corresponding control, and it was expressed as the percentage of viable cells. The IC_{50} was described as the concentration necessary to reach the mortality of 50% of cells.

Results and Discussion

Reduction of sodium selenite was clearly confirmed through observation with naked eye. A color change occurred, from colorless to a red solution within 15 min of reaction (Figure 1). This red coloring, which is characteristic of monoclinic colloidal selenium nanoparticles (a-SeNPs), is due to surface plasmon excitation.³⁸ Within 20 min of reaction, black coloring nanoparticles were obtained, which is characteristic of selenium nanoparticles in the trigonal phase (t-SeNPs).³⁹

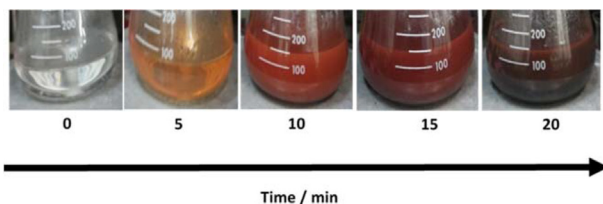


Figure 1. Selenium nanoparticles formation: reaction as a function of time.

Figure 2a shows the XRD pattern of the sample obtained after 15 min of reaction, which has no sharp peak, confirming that the selenium nanoparticles synthesized under these conditions were in the amorphous phase (a-SeNPs).²⁴ In the sample obtained after 20 min of reaction, peaks were observed (Figure 2b) at $2\theta = 23, 29, 41, 43, 45, 51, 55, 61$ and 65° , corresponding to the crystalline planes 100, 101, 110, 102, 111, 201, 112, 103. All the peaks could be indexed to the trigonal phase of selenium nanoparticles (t-SeNPs).⁴⁰ The lattice constants of $a = 4.3662 \text{ \AA}$ and $c = 4.9521 \text{ \AA}$ are consistent with the standard values for bulk Se with $a = 4.3662 \text{ \AA}$ and $c = 4.9536 \text{ \AA}$, according to JCPDS file No. 73-0465.

The HRTEM images corroborate the X-ray diffraction data, which show selenium nanoparticles obtained at 15 min of the reaction having spherical shape without aggregation of particles (Figures 3A and 3B). This is characteristic of the amorphous phase^{30,31} (a-SeNPs) with the size ranging between 80-100 nm, and average particle size at 80 nm (Figures 3A and 3B). Figures 3C and 3D show that the shape of the nanoparticle depends on the reaction time.

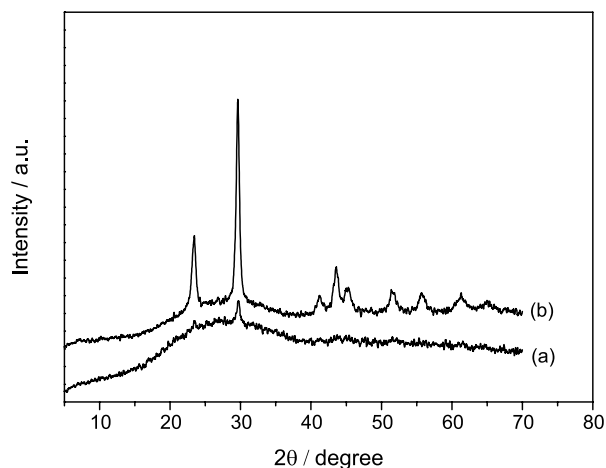


Figure 2. XRD pattern of selenium nanoparticles prepared using *D*-fructose after 15 min reaction, a-SeNPs (a), and after 20 min reaction, t-SeNPs (b).

After 20 min of reaction, the amorphous Se spheres (a-SeNPs) tend to form aggregates. Then, the particles start crystallization presenting rod-like shape, which can be characteristic of t-SeNPs.³⁰ This behavior was observed in other studies in which conventional methods of synthesis of selenium nanoparticles were used.²⁴

The EDX analysis shows qualitatively and quantitatively the elements that may be involved in the formation of nanoparticles. Figure 4 shows the high purity of the selenium nanoparticles synthesized. The two peaks at 11.2 and 12.1 keV, are related to the presence of selenium.³¹

The nanoparticle stability is very important for a number of applications, and can be determined through the zeta potential. For a-SeNPs synthesized in this work, the zeta potential was found to be $-27.8 \pm 0.5 \text{ mV}$. This result indicates the high stability of monodisperse nanoparticles.^{32,41} To the nanoparticles obtained after 20 min of reaction, t-SeNPs, the measured zeta potential was $-18.2 \pm 0.9 \text{ mV}$. This confirms the results obtained by the HRTEM image, which showed polydisperse particle aggregation, and indicates the poor stability of them.

Figure 5 compares the voltammetric responses of nanoparticulate deposits of a-SeNPs and t-SeNPs attached to graphite immersed into 0.25 mol L^{-1} HAc/NaAc aqueous buffer. Using square wave voltammetry as a detection mode, both oxidation and reduction signals can be seen in positive-going scans. Upon scanning the potential from $-0.85 \text{ V vs. Ag/AgCl}$ in the positive direction, the a-SeNPs displayed voltammetric signals at $-0.80, -0.20$ and a shoulder at $+0.95 \text{ V}$. Remarkably, the t-SeNPs produced weaker shoulders at $-0.80, -0.20$ and $+0.10 \text{ V}$ intercalated between a sharp peak at -0.45 and a broad wave at $+0.95 \text{ V}$. These responses can be interpreted in terms of the occurrence of two different electrochemical

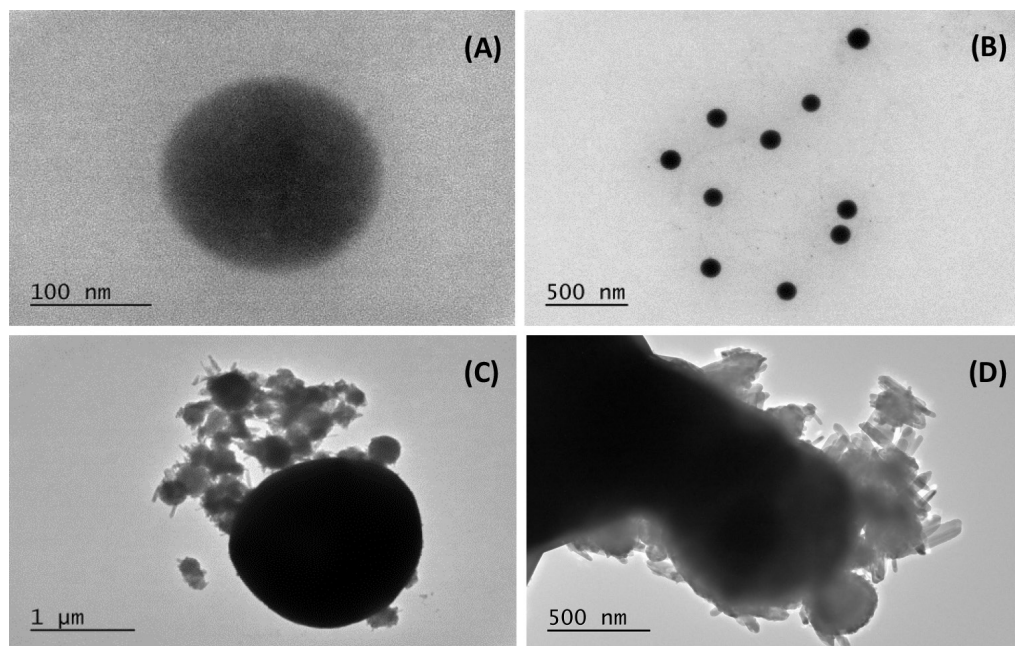


Figure 3. HRTEM images of the transformation process of a-SeNPs nanospheres to t-SeNPs nanorods. (A) a-SeNPs individual nanosphere ; (B) uniform nanospheres of a-SeNPs; (C) aggregation and beginning of the transformation into t-SeNPs nanorods; (D) nanorods aggregates of t-SeNPs.

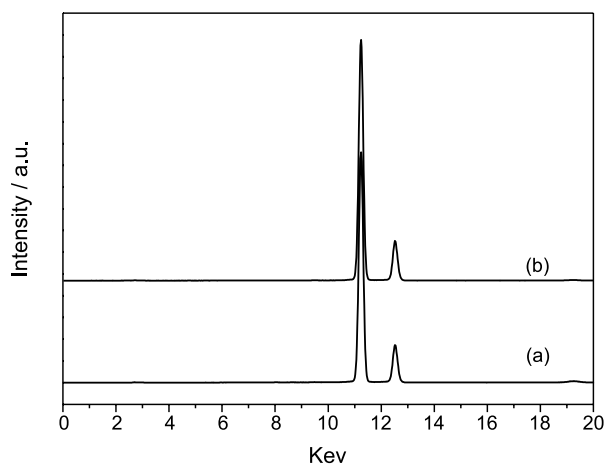


Figure 4. EDX spectrum of a-SeNPs after 15 min reaction (a) and t-SeNPs after 20 min (b).

pathways. First of all, the common signal at -0.80 V can be attributed to the reduction of Se to H_2Se .⁴² The oxidation of SeNPs, however, occurs differently for a- and t-SeNPs. In this second case, a sharp signal at -0.45 V appears, corresponding to a typical stripping process⁴³ due to the oxidation of selenium(0) to selenium(II) species in solution. In contrast, the oxidation of a-SeNPs gives rise to a broad peak at -0.20 V which can be attributed to the selenium(0) oxidation to NP-associated selenium(II). Such processes would precede the oxidation of selenium(0) and selenium(II) to selenium(IV), producing the oxidation signals at more positive potentials.⁴⁴⁻⁴⁶

These features can be rationalized assuming that selenium(0) oxidation is quite sensitive to the crystalline

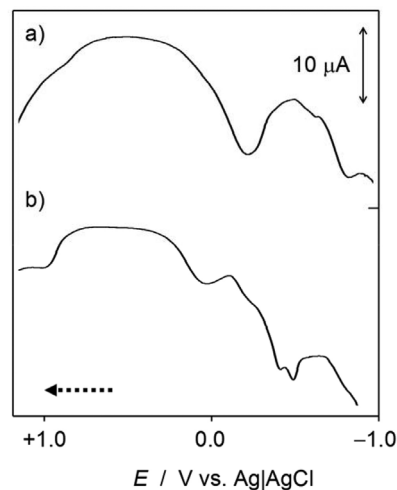


Figure 5. Square wave voltammograms of nanoparticulate deposits of: (a) a-SeNPs and (b) t-SeNPs attached to graphite electrode, immersed into 0.25 mol L^{-1} HAC/NaAc buffer solution. Potential scan initiated at -0.85 V, in the positive direction. Potential step increment, 4 mV; square wave amplitude, 25 mV; frequency, 5 Hz.

structure, as observed in the electrochemistry of, for instance, gold NPs.^{47,48} In the case of t-SeNPs, which have a rigid structural arrangement, the electrochemical oxidation is dominated by the process at -0.45 V which yields mainly selenium(II) in solution. In contrast, the oxidation of a-SeNPs, where a more flexible coordinative environment for Se atoms exists, can result in a smoother oxidation (process at -0.20 V), producing selenium(II) species associated to the NP. In summary, the availability of electroactive sites cycling between the selenium(0) and selenium(II) states is the key difference between the a- and t-SeNPs.

Cytotoxicity data

The colloidal selenium nanoparticles a-SeNPs, obtained after 15 min of reaction, were evaluated for potential antitumor cytotoxicity against the cell line of uterine cancer MES-SA/Dx5 (doxorubicin-resistant mutants, with P-gp overexpression), and its parental cell line MES-SA. In addition, they were also tested for fibroblasts cell line P4. As shown in Figure 6A, the a-SeNPs were not able to affect P4 cells significantly, since the observed cell viability was 98 and 85% after 24 and 48 h of incubation, respectively, at a concentration of 140 μM . This data indicates that the selenium nanoparticles are non-toxic for this type of human healthy cell. In contrast, the results for cancer cells, shown in Figures 6B and 6C indicate that a-SeNPs present high toxicity with respect to the sarcoma cells. Cell viability decreases gradually with increasing concentration, and the activity is higher with increasing incubation time, for both cancer cell lines studied. IC_{50} values were very similar, 110.01 ± 0.23 and 80.12 ± 0.41 μM , at 24 and 48 h, respectively, for

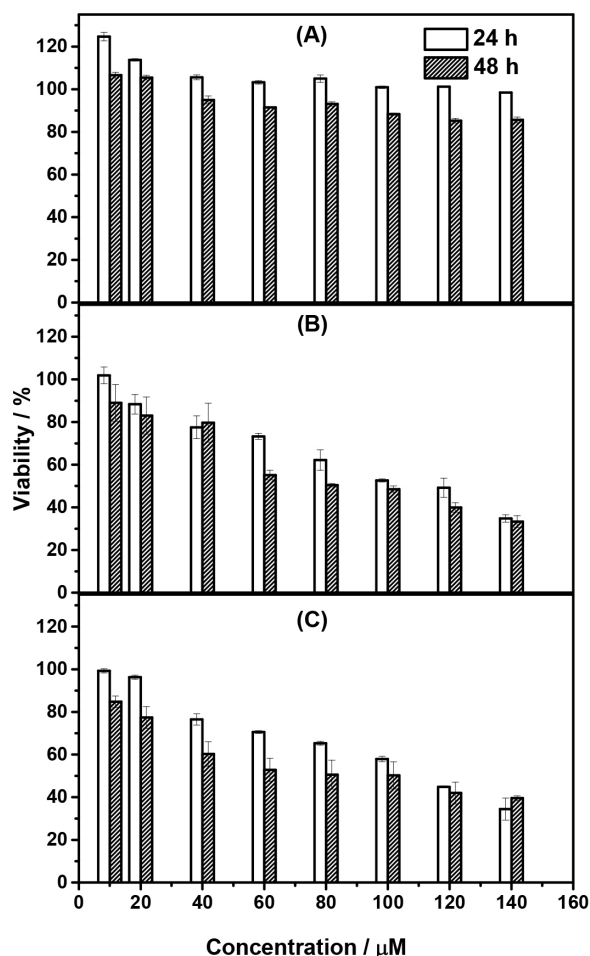


Figure 6. Effect of a-SeNPs synthesized by reduction with *D*-fructose on the viability of (A) P4 cell lines; (B) MES-SA cells and (C) MES-SA/Dx5.

MES-SA and 110.19 ± 0.12 and 81.38 ± 0.34 μM , at 24 and 48 h, respectively, for MES-SA/Dx5. The MES-SA/Dx5 cells usually overexpress P-glycoproteins, which act as a drug efflux pump. Consequently, these cells require higher doses of cytotoxic agent in comparison to the non-resistant cells.⁴⁹ Therefore, these results show that the nanoparticles are equally toxic toward both the MDR (MES-SA/Dx5) and the non-resistant (MES-SA) cancer cell lines. This makes a-SeNPs a promising candidate to pharmaceutical agents to overcome resistance in cancer cells.

A previous study in the literature⁵⁰ showed that SeNPs coupled with adenosine triphosphate (ATP, 2.5-40 μM) inhibit the cellular viability of hepatocellular cancer strain (HepG2), but do not exhibit toxicity to normal human kidney cells (HK-2). In a more recent paper,⁵¹ SeNPs were applied to HCT-8 cells (ileocecal adenocarcinoma), indicating that after 48 h of treatment only 27% of the cells survive, when 200 μM of SeNPs were used. Associated with irinotecan, SeNPs are able to inhibit the growth of this strain more efficiently compared to each irinotecan or SeNPs alone. Concerning normal cells (IEC6), the SeNPs were less toxic than irinotecan.⁵¹ Breast cancer cells (MCF-7 and MDA-MB-231) were also treated with SeNPs, and an IC_{50} value of 25 $\mu\text{g mL}^{-1}$ was obtained *versus* the MCF-7 line. For the MDA-MB-231 cell line, the inhibition was only 33% when the same maximum concentration was used, suggesting that SeNPs possess greater selectivity for early stage breast cancer compared to the metastatic breast cancer cells (MDA-MB-231).³³ SeNPs (10-40 μM) synthesized using vitamin C also showed activity against the lines MDA-MB-231 and HeLa (human cervical carcinoma). The viability of MDA-MB-231 cells was decreased to 60% and of HeLa cells was reduced between 73 and 50%, in the presence of Se-NPs.⁵² This is the first time that MES-SA and MES-SA/Dx5 cell lines are tested in studies with selenium nanoparticles. The obtained results confirmed the overall trends reported in the literature. As here discussed, SeNPs have great potential in the treatment against cancer cells, due mainly to its low toxicity toward normal cells. In addition, these results are quite attractive in terms of selectivity, since SeNPs were capable of inducing the mortality of MDR tumor cells (MES-SA/Dox5), which overexpress the glycoprotein P-gp responsible for the efflux effect in tumor cells, at the same intensity as compared with the standard MES-SA cells (Table 1).

Conclusions

In this study, we described a “green” synthesis of SeNPs using *D*-fructose as a reducing agent, by a simple, economic and fast process. This is the first report of

Table 1. Cytotoxicity of SeNPs against different cell lines

Cell line	Incubation time / h	IC ₅₀ / μM	Size average diameter / nm	Reference
Normal				
HK-2	24	> 40	1000	50
IEC6	48	non-toxic	20	51
P4	24 and 48	> 140	80	this work
Cancer				
HepG2	24	ca. 7.5	1000	50
HCT-8	48	ca. 50	20	51
MCF-7	24	310	150	33
MDA-MB-231	24	1265	150	33
MDA-MB-231	24	> 506	133	52
HeLa	24	> 506	133	52
MES-SA	48	80	80	this work
MES-SA/Dx5	48	80	80	this work

IC₅₀: the concentration necessary to reach the mortality of 50% of cells.

synthesis of Se nanoparticles where *D*-fructose has been used. Characterization techniques used indicate that at 15 min of reaction colloidal nanoparticles (a-SeNPs) were obtained, and in 20 minutes the process of transformation of a-SeNPs to t-SeNPs starts. HRTEM showed that a-SeNPs were obtained with 80 nm average particle size. Their purity was confirmed by EDX. Further, the a-SeNPs are highly stable with determined zeta potential of $(-27.8 \pm 0.5 \text{ mV})$. These data indicate that the electron transfer ability of the a-SeNPs and t-SeNPs nanoparticles is clearly different. Those results are in agreement with the observed cytotoxic data, since selenium nanoparticles induce pronounced death of cancer cells (MES-SA/Dx5 and MES-SA cells), but did not show noticeable antiproliferative effects on fibroblasts cells (P4) growth. These results indicate that SeNPs can be good candidates as new therapeutic drugs for uterine cancer treatment.

Acknowledgments

Financial support from the Brazilian entities Coordenação de Aperfeiçoamento de Pessoal de Nível Superior (CAPES), São Paulo State Research Foundation (FAPESP), the Ministerio de Ciencia e Innovación (MICIN) Project CTQ2014-53736-C3-2-P, which is also supported with European Regional Development Funds, is gratefully acknowledged.

References

1. Rayman, M. P.; *Lancet* **2000**, 356, 233.

- Comasseto, J. V.; *J. Braz. Chem. Soc.* **2010**, 21, 2027.
- Bao, Y. P.; Williamson, G.; *Prog. Nat. Sci.* **2000**, 10, 321.
- Shen, H. M.; Yang, C. F.; Ding, W. X.; Liu, J.; Ong, C. N.; *Free Radical Biol. Med.* **2001**, 30, 9.
- Sinha, R.; Ei-Bayoumy, K.; *Curr. Cancer Drug Targets* **2004**, 4, 13.
- Ellis, R. D.; Salt, E. D.; *Curr. Opin. Plant Biol.* **2003**, 6, 273.
- Tapiero, H.; Townsend, D. M.; Tew, K. D.; *Biomed. Pharmacother.* **2003**, 57, 134.
- Abdulah, R.; Miyazaki, K.; Nakazawa, M.; Koyama, H.; *J. Trace Elem. Med. Biol.* **2005**, 19, 141.
- Huang, B.; Zhang, J. S.; Hou, J. W.; Chen, C.; *Free Radical Biol. Med.* **2003**, 35, 805.
- Wang, H. L.; Zhang, J. S.; Yu, H. Q.; *Free Radical Biol. Med.* **2007**, 42, 1524.
- Tarze, A.; Dauplais, M.; Grigoras, I.; Lazard, M.; Ha-Duong, N. T.; Barbier, F.; Blanquet, S.; Plateau, P.; *J. Biol. Chem.* **2007**, 282, 8759.
- Zhang, J. S.; Wang, H. L.; Yan, X. X.; Zhang, L. D.; *Life Sci.* **2005**, 76, 1099.
- Peng, D.; Zhang, J.; Liu, Q.; Taylor, E. W.; *J. Inorg. Biochem.* **2007**, 101, 1457.
- Zhou, X. X.; Wang, Y. B.; Gu, Q.; Li, W. F.; *Aquaculture* **2009**, 291, 291.
- Acharya, S.; Dilnawaz, F.; Sahoo, S. K.; *Biomaterials* **2009**, 30, 5737.
- Patra, H. K.; Banerjee, S.; Chaudhuri, U.; Lahiri, P.; Dasgupta, A. K.; *Nanomedicine* **2007**, 3, 111.
- Durán, N.; Marcato, P. D.; de Conti, R.; Alves, O. L.; Costa, F. T. M.; Brocchi, M.; *J. Braz. Chem. Soc.* **2010**, 21, 949.
- Wadhvani, S. A.; Shedbalkar, U. U.; Singh, R.; Chopade, B. A.; *Appl. Microbiol. Biotechnol.* **2016**, 100, 2555.
- Cao, X. B.; Xie, Y.; Li, L. Y.; *Adv. Mater.* **2003**, 15, 1914.
- Ma, Y. R.; Qi, L. M.; Shen, W.; Ma, J. M.; *Langmuir* **2005**, 21, 6161.
- Chen, Z. X.; Shen, Y. H.; Xie, A. J.; Zhu, J. M.; Wu, Z. F.; Huang, F. Z.; *Cryst. Growth Des.* **2009**, 9, 1327.
- Yang, L. B.; Shen, Y. H.; Xie, A. J.; Liang, J. J.; *Eur. J. Inorg. Chem.* **2007**, 4438.
- Li, S. K.; Shen, Y. H.; Xie, A. J.; Yu, X. Y.; Zhang, X. Z.; Yang, L. B.; Li, C. H.; *Nanotechnology* **2007**, 18, 405101.
- Song, J. M.; Zhu, J. H.; Yu, S. H.; *J. Phys. Chem. B* **2006**, 110, 23790.
- Quintana, M.; Haro-Poniatowski, E.; Morales, J.; Batina, N.; *Appl. Surf. Sci.* **2002**, 195, 175.
- Wang, M. C. P.; Zhang, X.; Majidi, E.; Nedelec, K.; Gates, B. D.; *ACS Nano* **2010**, 4, 2607.
- Filippo, E.; Manno, D.; Serra, A.; *Cryst. Growth Des.* **2010**, 10, 4890.
- Avendaño, R.; Chaves, N.; Fuentes, P.; Sánchez, E.; Jiménez, J. I.; Chavarría, M.; *Sci. Rep.* **2016**, 6, 37155.

29. Wang, T.; Yang, L.; Zhang, B.; Liu, J.; *Colloids Surf., B* **2010**, *80*, 94.
30. Zhang, W.; Chen, Z.; Liu, H.; Zhang, L.; Gao, P.; Li, D.; *Colloids Surf., B* **2011**, *88*, 196.
31. Prasad, K. S.; Patel, H.; Patel, T.; Patel, K.; Selvaraj, K.; *Colloids Surf., B* **2013**, *103*, 261.
32. Zhang, S.-Y.; Zhang, J.; Wang, H.-Y.; Chena, H.-Y.; *Mater. Lett.* **2004**, *58*, 2590.
33. Vekariya, K. K.; Kaur, J.; Tikoo, K.; *Nanomedicine* **2012**, *8*, 1125.
34. Nie, T.; Wu, H.; Wong, K.-H.; Chen, T.; *J. Mater. Chem. B* **2016**, *4*, 2351.
35. Chen, H.; Yoo, J.-B.; Liu, Y.; Zhao, G.; *Electron. Mater. Lett.* **2011**, *7*, 333.
36. Chen, H.; Shin, D.-W.; Nam, J.-G.; Kwon, K.-W.; Yoo, J.-B.; *Mater. Res. Bull.* **2010**, *45*, 699.
37. Denizot, F.; Lang, R.; *J. Immunol. Methods* **1986**, *89*, 271.
38. Lin, Z. H.; Wang, C. R. C.; *Mater. Chem. Phys.* **2005**, *92*, 591.
39. Zhang, J. S.; Wang, H. L.; Bao, Y. P.; Zhang, L.; *Life Sci.* **2004**, *75*, 237.
40. Gates, B.; Mayers, B.; Cattle, B.; Xia, Y.; *Adv. Funct. Mater.* **2002**, *12*, 219.
41. Kong, H.; Yang, J.; Zhang, Y.; Fang, Y.; Nishinaria, K.; Phillips, G. O.; *Int. J. Biol. Macromol.* **2014**, *65*, 155.
42. Santos, M. C.; Machado, S. A. S.; *J. Electroanal. Chem.* **2004**, *567*, 203.
43. Lovric, M. In *Electroanalytical Methods*; Scholz, F., ed.; Springer: Berlin, 2002.
44. Beni, V.; Collins, G.; Arrigan, D. W. M.; *Anal. Chim. Acta* **2011**, *699*, 127.
45. Fierro, S.; Watanabe, T.; Akai, K.; Yamanuki, M.; Einaga, Y.; *Int. J. Electrochem.* **2012**, 758708.
46. Feng, Y.; Gu, M.; *Electrochim. Acta* **2013**, *90*, 416.
47. Chen, A.; Lipkowski, J.; *J. Phys. Chem. B* **1999**, *103*, 682.
48. Burke, L. D.; O'Mullane, A. P.; *J. Solid State Electrochem.* **2000**, *4*, 285.
49. Vieira, A. P.; Stein, E. M.; Andregueti, D. X.; Colepicolo, P.; Ferreira, A. M. C.; *J. Appl. Physiol.* **2016**, *28*, 2615.
50. Zhang, Y.; Li, X.; Huang, Z.; Zheng, W.; Fan, C.; Chen, T.; *Nanomedicine* **2013**, *9*, 74.
51. Gao, F.; Yuan, Q.; Gao, L.; Cai, P.; Zhu, H.; Liu, R.; Wang, Y.; Wei, Y.; Huang, G.; Liang, J.; Gao, X.; *Biomaterials* **2014**, *35*, 8854.
52. Luo, H.; Wang, F.; Baia, Y.; Chen, T.; Zheng, W.; *Colloids Surf., B* **2012**, *94*, 304.

Submitted: August 26, 2016

Published online: February 13, 2017